Supplementary Data:

S1: Spectra of Microplastics and Cellulose in Gelatin:

Three individual spectra and their corresponding mean spectrum from three different particles of several materials embedded in phantoms are shown in Supplementary Figure S1. The materials investigated included the MPs polyamide (PA), polyethylene (PE), polystyrene (PS), and polypropylene (PP), the MFs PP and polytetrafluoroethylene (PTFE), and cellulose microparticles. Variation in spectral features is apparent, which can arise for several reasons. Scattering can occur due to the spherical shape of microplastic particles (MPs) and the circular cross-section of microplastic fibers (MFs) which may account for the differences in spectral features. Additionally, some spectra may have a gelatin phantom material contribution in addition to the MF or MP characteristic bands if a small amount of gelatin is covering the particle. Moreover, orientation of the polymer in the sample and the direction of the polarized IR laser source radiation can affect absorbance bands, and this may be particularly evident in Amide I and Amide II absorbances, such as in Nylon (polyamide, PA). The laser source radiation in the mIRage spectrometer is inherently polarized along the X axis of the sample stage, and when the Amide II vibration (a mixture of N-H bending and C-N stretching, between 1500-1600 cm^{-1}, aligned with the fiber axis) has the same orientation as the polarized IR radiation, this phenomenon is apparent. (Supplementary Figure 2-A and C). A similar situation can occur when the polarized IR radiation is in the direction of the Amide I vibration (C=O stretch, between 1600-1700 cm^{-1}) which is perpendicular to fiber axis, there will be greater absorbance of IR radiation and a greater peak area/height (Supplementary Figure S1-B).

Another notable observation in the OPTIR spectra is the slight shift in characteristic peak positions across different compounds, such as PA MP, cellulose, PS MP, and PTFE MF. This shift can be caused by scattering, polymer orientation or matrix absorbance effect.

Supplementary Figure S1. Individual spectrum (n=3) and mean spectrum from three different particles embedded in the phantom. A, B, and C: Nylon- PA MP; D, E, and F: Cellulose; G, H, and I: PE MP; J, K, and L: PP MP; M, N, and O: PP MF; P, Q, and R: PS MP; S, T, and U: PTFE MF.

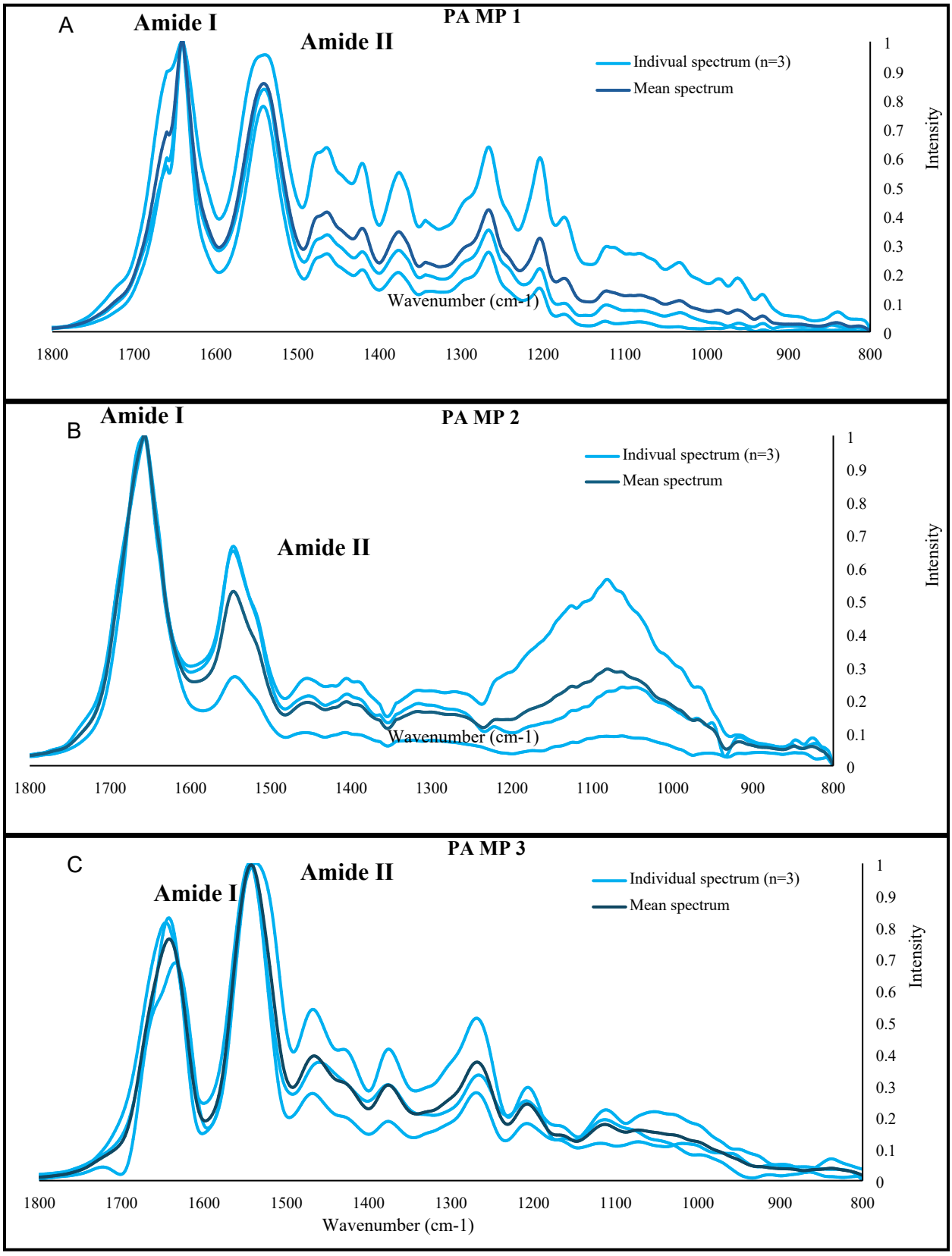
A
Amide I
Amide II
PA MP 1
Indivual spectrum (n=3)
Mean spectrum
Intensity
Wavenumber (cm-1)
1800 1700 1600 1500 1400 1300 1200 1100 1000 900 800
0 0.1 0.2 0.3 0.4 0.5 0.6 0.7 0.8 0.9 1
B
Amide I
Amide II
PA MP 2
Indivual spectrum (n=3)
Mean spectrum
Intensity
Wavenumber (cm-1)
1800 1700 1600 1500 1400 1300 1200 1100 1000 900 800
0 0.1 0.2 0.3 0.4 0.5 0.6 0.7 0.8 0.9 1
C
Amide I
Amide II
PA MP 3
Individual spectrum (n=3)
Mean spectrum
Intensity
Wavenumber (cm-1)
1800 1700 1600 1500 1400 1300 1200 1100 1000 900 800
0 0.1 0.2 0.3 0.4 0.5 0.6 0.7 0.8 0.9 1

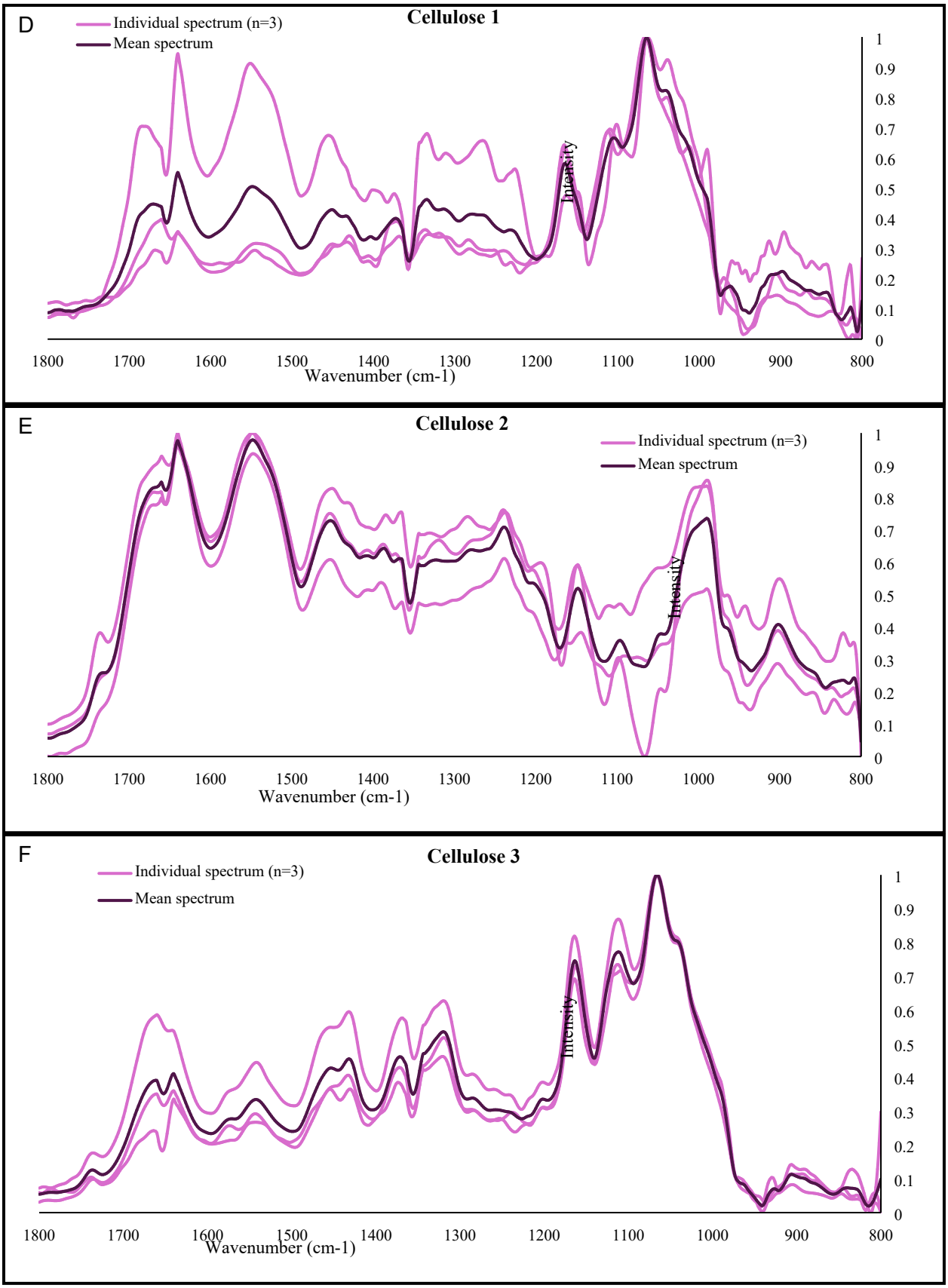
D
Cellulose 1
Individual spectrum (n=3)
Mean spectrum
Intensity
1
0.9
0.8
0.7
0.6
0.5
0.4
0.3
0.2
0.1
0
1800
1700
1600
1500
1400
1300
1200
1100
1000
900
800
Wavenumber (cm-1)
E
Cellulose 2
Individual spectrum (n=3)
Mean spectrum
Intensity
Wavenumber (cm-1)
F
Cellulose 3
Individual spectrum (n=3)
Mean spectrum
Intensity
Wavenumber (cm-1)

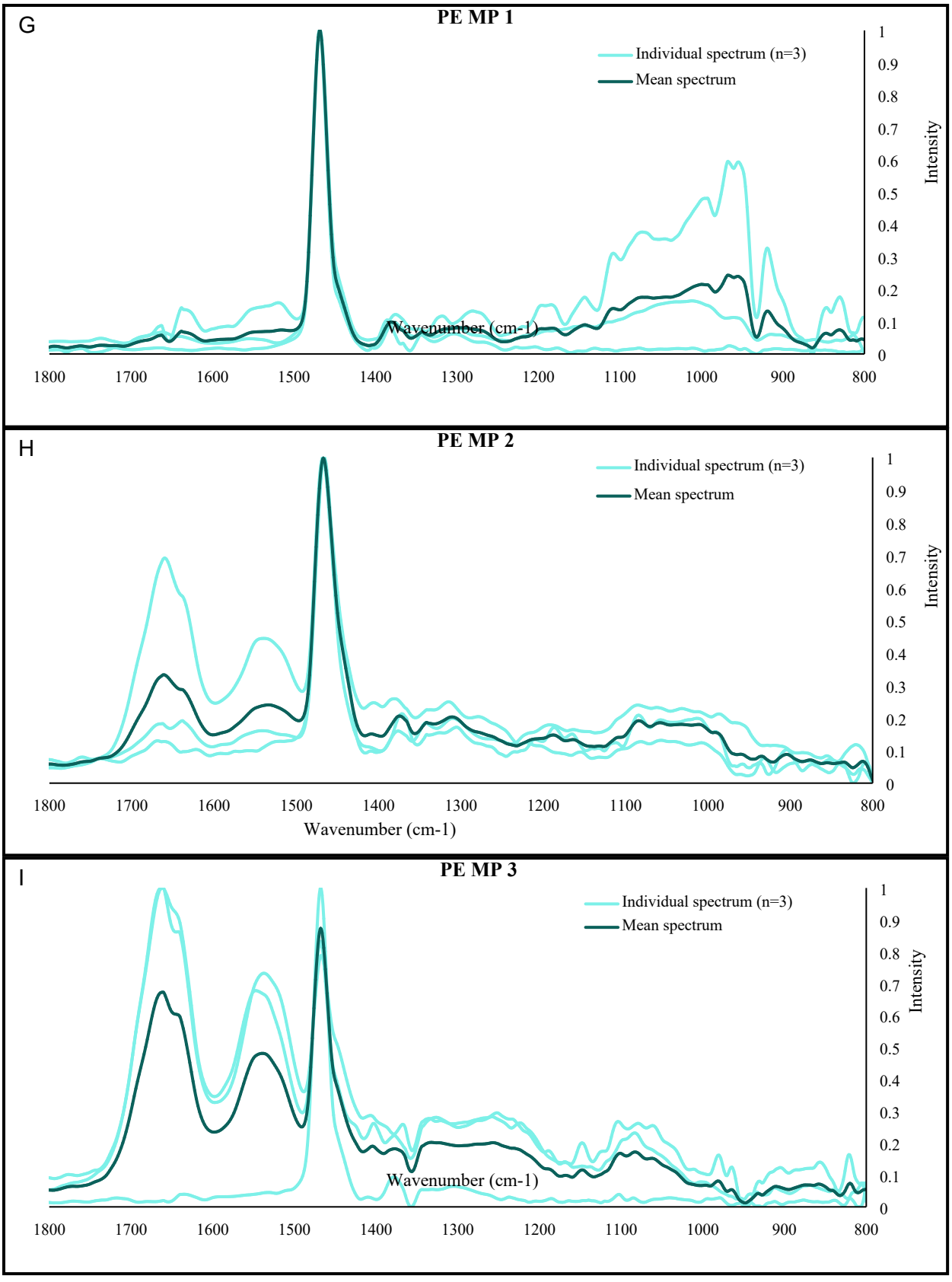
G
PE MP 1
Individual spectrum (n=3)
Mean spectrum
Intensity
Wavenumber (cm-1)
1800 1700 1600 1500 1400 1300 1200 1100 1000 900 800
0 0.1 0.2 0.3 0.4 0.5 0.6 0.7 0.8 0.9 1
H
PE MP 2
Individual spectrum (n=3)
Mean spectrum
Intensity
Wavenumber (cm-1)
1800 1700 1600 1500 1400 1300 1200 1100 1000 900 800
0 0.1 0.2 0.3 0.4 0.5 0.6 0.7 0.8 0.9 1
I
PE MP 3
Individual spectrum (n=3)
Mean spectrum
Intensity
Wavenumber (cm-1)
1800 1700 1600 1500 1400 1300 1200 1100 1000 900 800
0 0.1 0.2 0.3 0.4 0.5 0.6 0.7 0.8 0.9 1

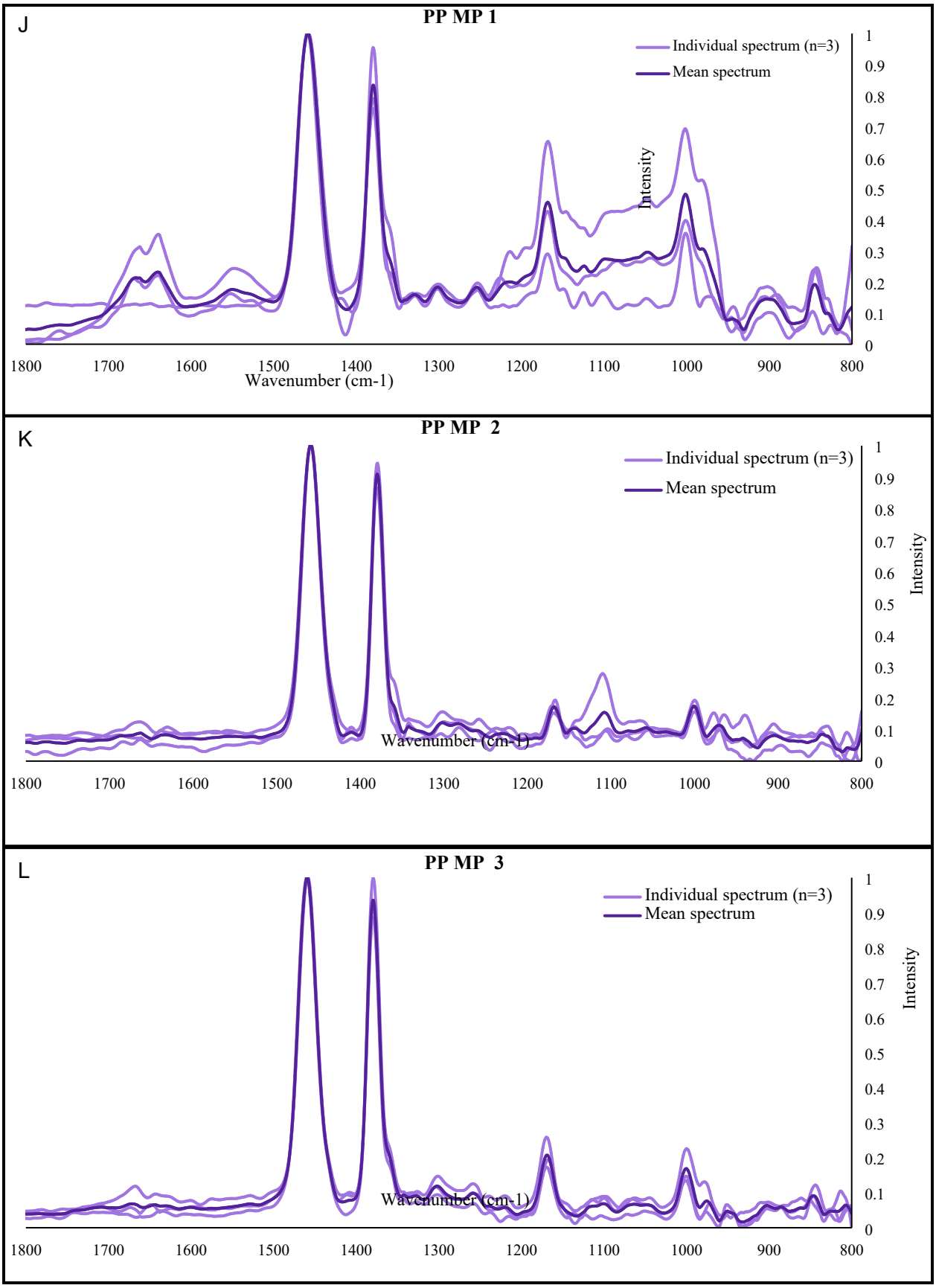
J
PP MP 1
Individual spectrum (n=3)
Mean spectrum
Intensity
Wavenumber (cm-1)
K
PP MP 2
Individual spectrum (n=3)
Mean spectrum
Intensity
Wavenumber (cm-1)
L
PP MP 3
Individual spectrum (n=3)
Mean spectrum
Intensity
Wavenumber (cm-1)

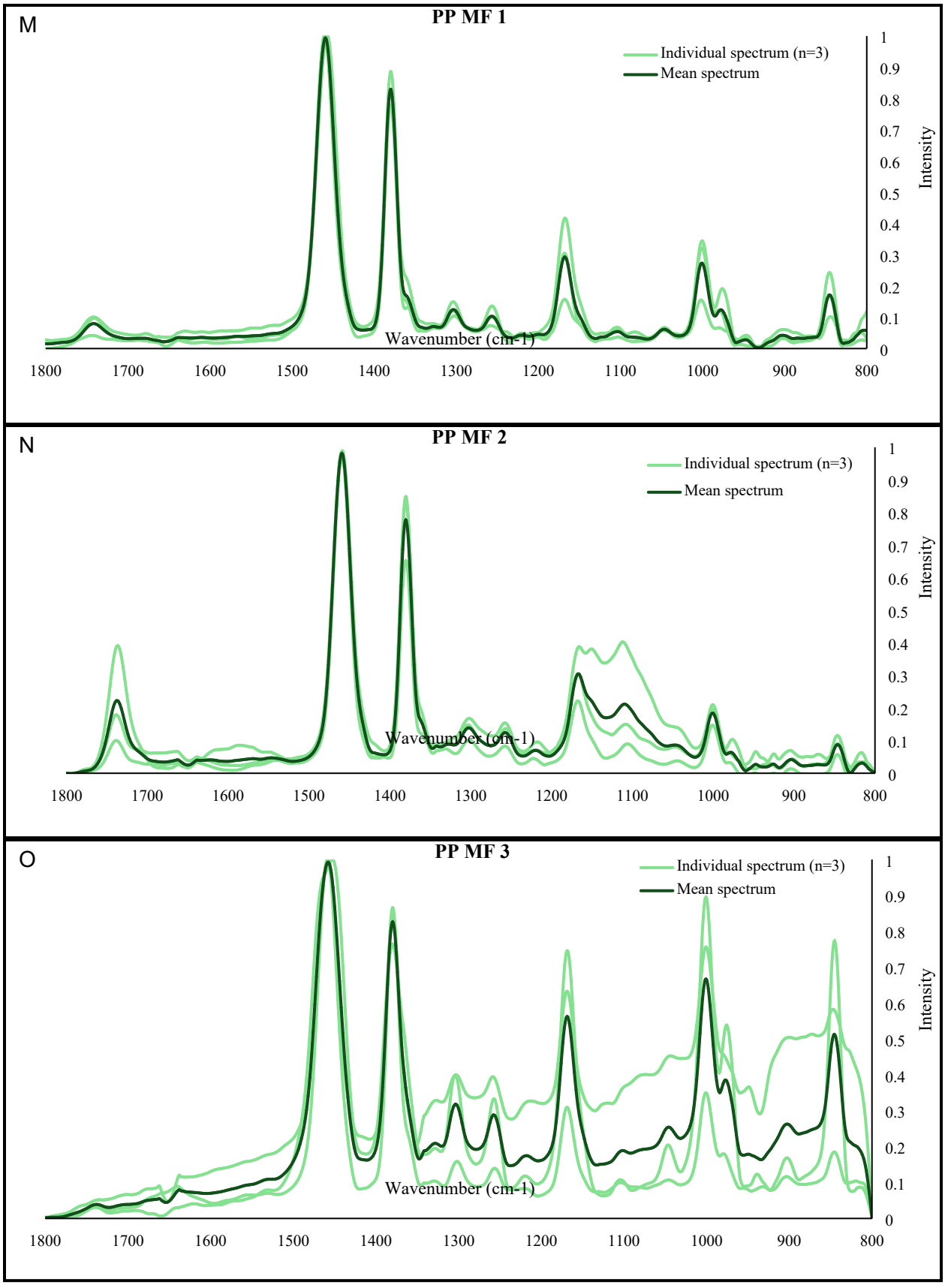
M
PP MF 1
Individual spectrum (n=3)
Mean spectrum
Intensity
Wavenumber (cm-1)
1800 1700 1600 1500 1400 1300 1200 1100 1000 900 800
0 0.1 0.2 0.3 0.4 0.5 0.6 0.7 0.8 0.9 1
N
PP MF 2
Individual spectrum (n=3)
Mean spectrum
Intensity
Wavenumber (cm-1)
1800 1700 1600 1500 1400 1300 1200 1100 1000 900 800
0 0.1 0.2 0.3 0.4 0.5 0.6 0.7 0.8 0.9 1
O
PP MF 3
Individual spectrum (n=3)
Mean spectrum
Intensity
Wavenumber (cm-1)
1800 1700 1600 1500 1400 1300 1200 1100 1000 900 800
0 0.1 0.2 0.3 0.4 0.5 0.6 0.7 0.8 0.9 1

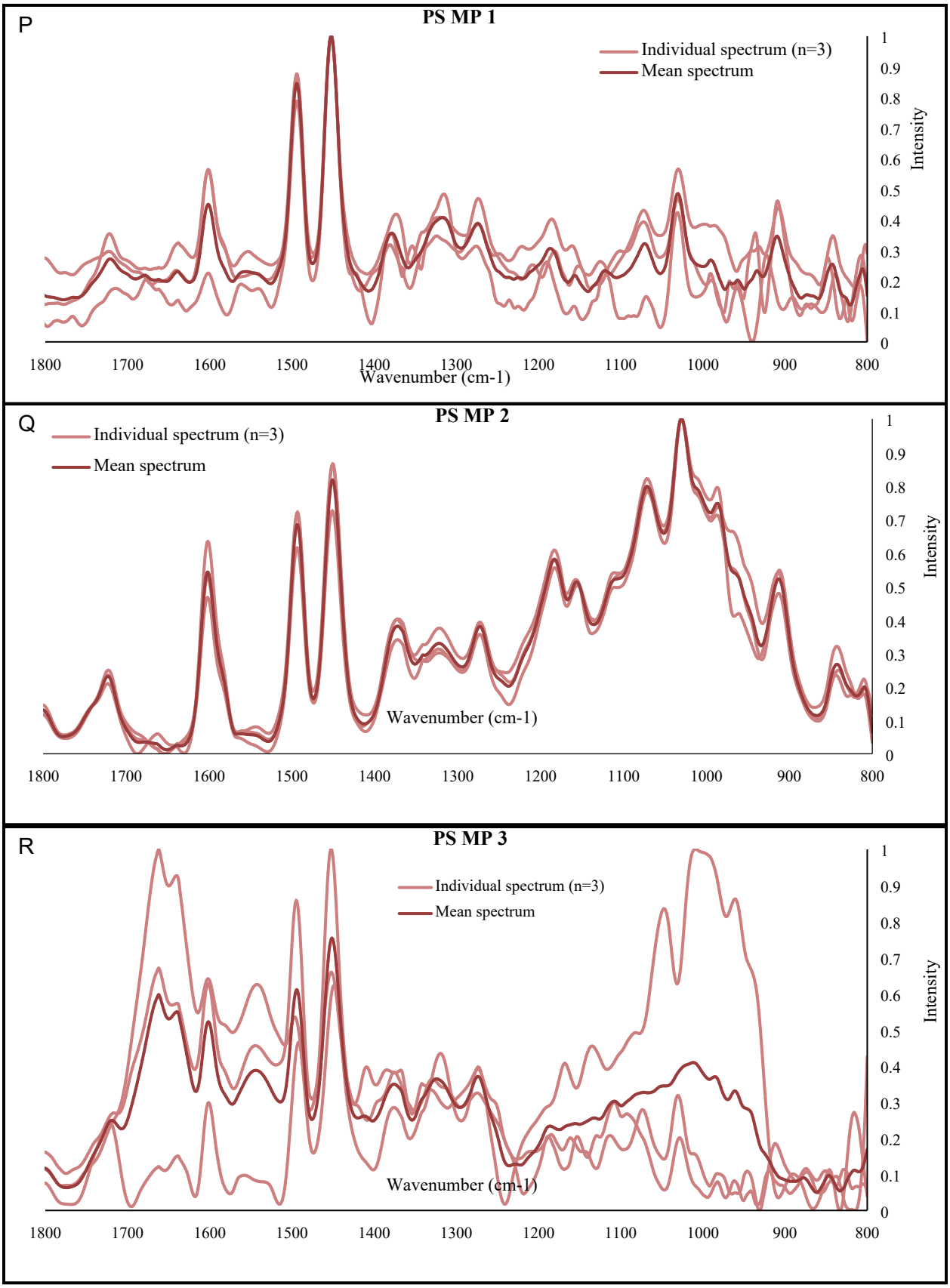
P
PS MP 1
Individual spectrum (n=3)
Mean spectrum
Intensity
Wavenumber (cm-1)
Q
PS MP 2
Individual spectrum (n=3)
Mean spectrum
Intensity
Wavenumber (cm-1)
R
PS MP 3
Individual spectrum (n=3)
Mean spectrum
Intensity
Wavenumber (cm-1)

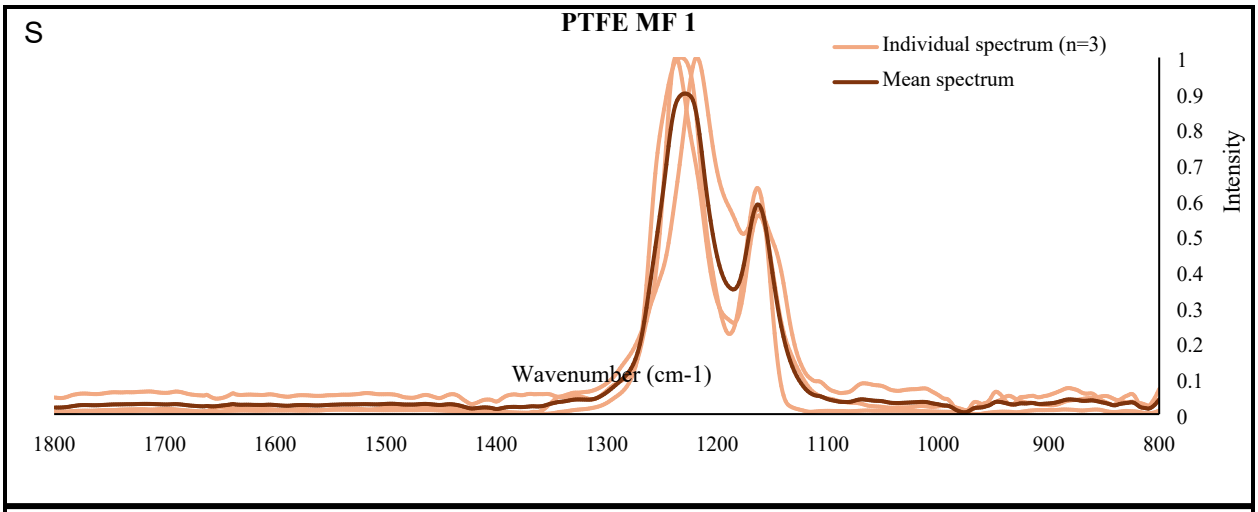

61

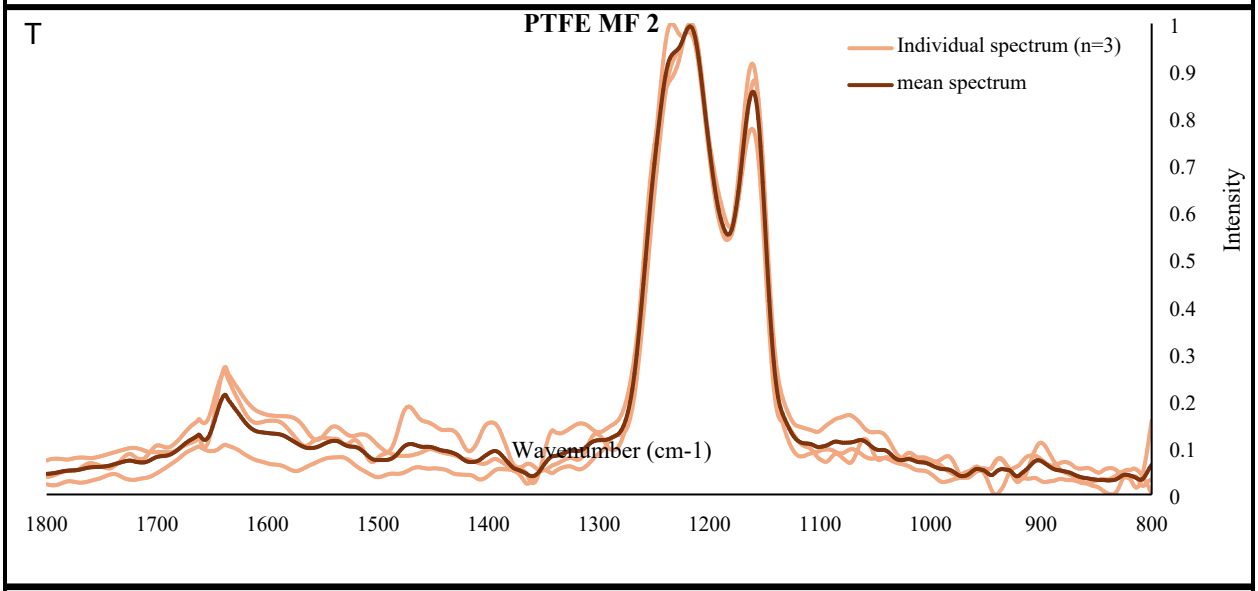

62

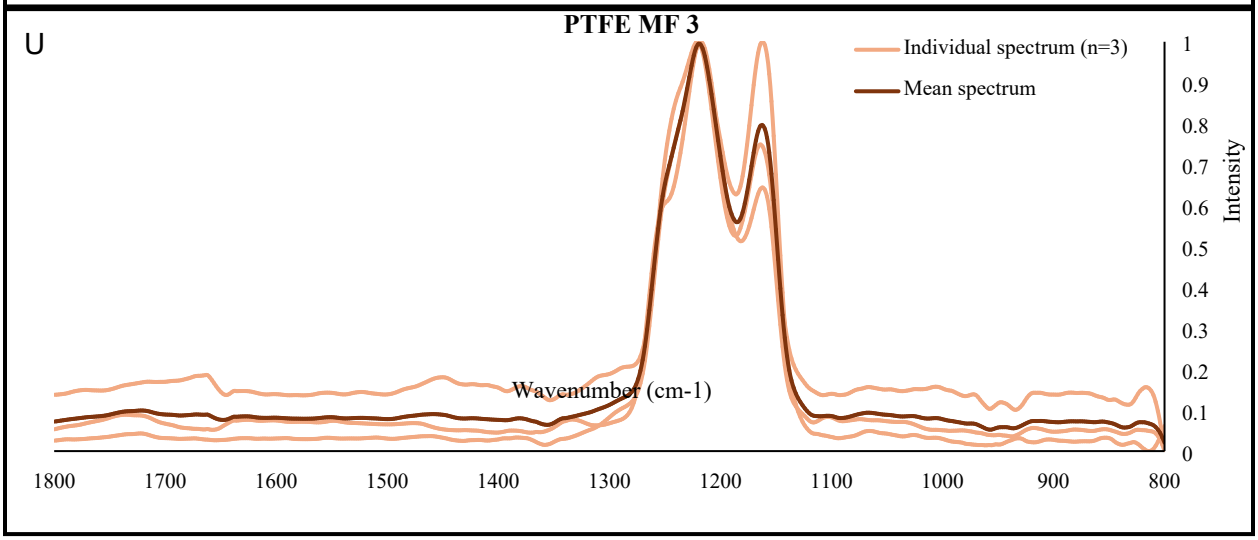

63
64
65
66

S2: Images and Spectra of a Contaminant in a Testis Tissue

A histological section from a human testis sample with no known disease/abnormality from the Cedars Sinai Medical Center Biobank (Los Angeles, CA) was formalin-fixed and paraffin-embedded and sectioned at six microns onto low-e slides (~25 mm^2). Although the embedding steps require contact with plastic molds, the sections of tissues evaluated came from the center of the sample and thus the paraffin edges with contact with plastic molds were avoided. IRB approval for use of this sample was not required as it was a de-identified tissue. Bright field (Figure S2A) and polarized light microscopy (PLM) images (Figure S2C) were collected from the sample and FTIR imaging data (Figure S2B) and O-PTIR data (Figure S3) were collected from a birefringent particle.

Features of the O-PTIR and FTIR spectra were similar, including the presence of the Amide I and Amide II absorbances, but there was a pronounced absorbance centered near ~ 1062 cm^{-1} in the O-PTIR spectra that was not present in the FTIR spectra (Figure S3C and D). Further, the FTIR spectra were more similar to the surrounding tissue spectra than were the O-PTIR spectra, indicative of contributions in the infrared signal from surrounding tissue. The average FTIR spectrum of the particle had percent matches ranging from 87- 89.6% with several proteins (collagen hydrolysate, Zein, human placenta extract) and Nylon -6; however, the 88% database match with Nylon 6 also supported the particle being birefringent, making it a likely match (Figure S3F). In contrast, the O-PTIR spectra exhibited the highest match with a composite spectrum that included Cascoloid ST-56, a casein-derived adhesive as the highest component (94.3%), (Figure S3E). It is unknown whether this adhesive would exhibit birefringence, which if it did not, it would rule it out as a match. There were also variations in O-PTIR spectra obtained from different regions of the particle with absorbances present at 1062, 1166, 1540, and 1650 cm^{-1} (Figure S3C). If the particle is indeed Nylon-6, the broad absorbance centered at around 1062 cm^{-1} indicates a structure modification, possibly by oxidation. Given that Nylon is a polyamide, the infrared absorbances (1166, 1540, and 1650 cm^{-1} reflecting CO-NH skeletal motion, amide II, N-H bend, C-N stretch, and amide I, C=O stretch (59–61))re present in many proteins, and certainly contribute to challenges in identifying Nylon in non-digested biological tissues. Thus, identification of this particle is not definitive.

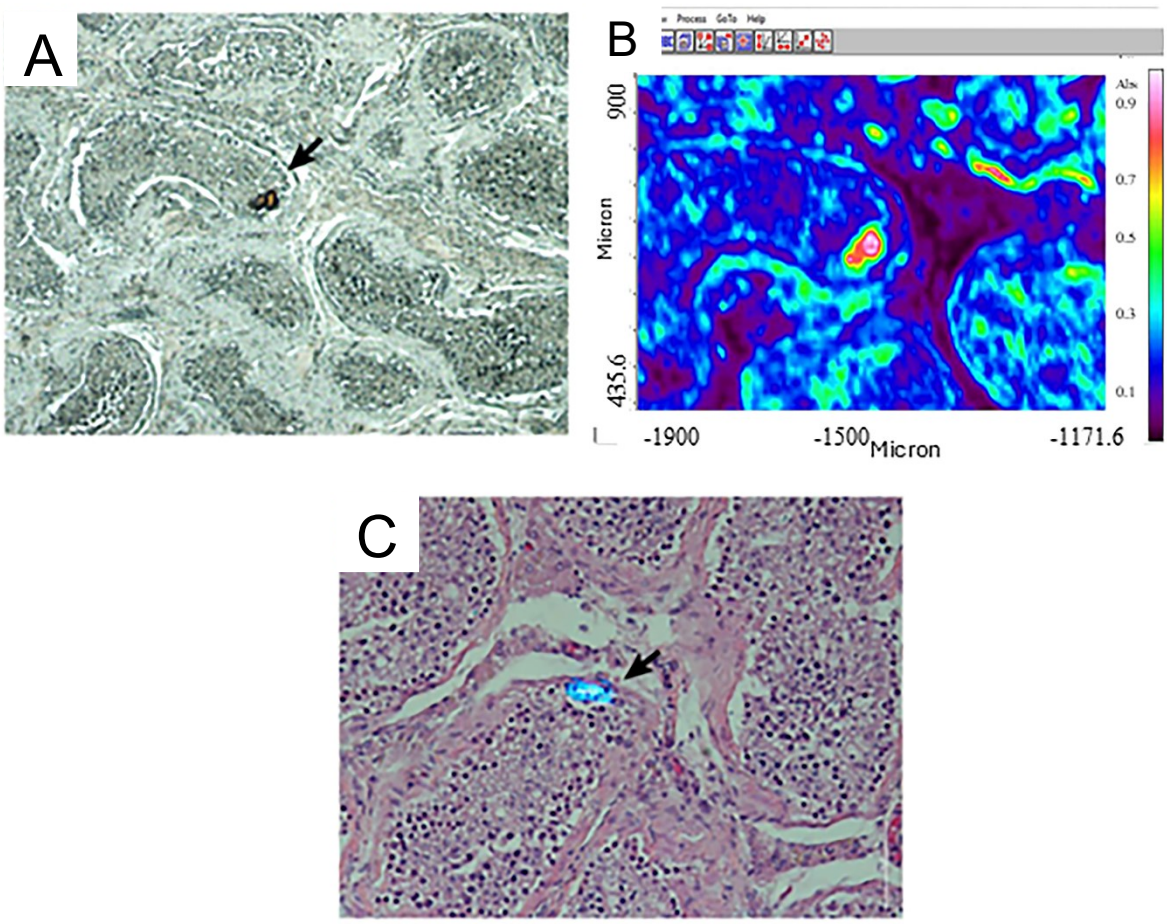

Supplementary Figure S2. Images from contaminants in testis tissue. **A.** A particle observed by bright-field microscopy in an unstained tissue. **B.** FTIR spectral image showing the absorbance map of the particle at 1650 cm^{-1}. **C.** Stained tissue sample showing the same particle as in A and B, viewed under polarized light in a slightly different orientation.

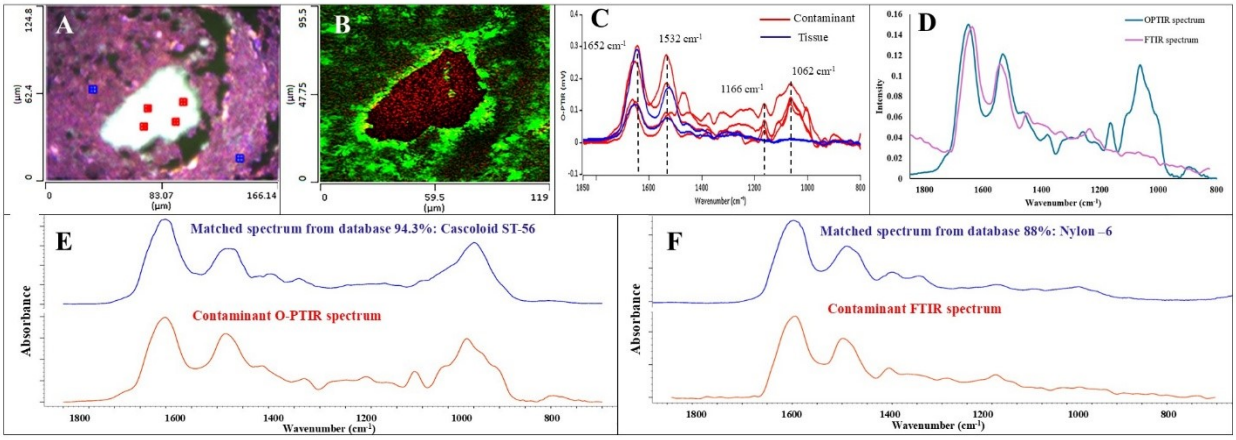

Figure S3: Images and O-PTIR spectra from contaminant in testis tissue. **A.** O-PTIR visible image of a contaminant in the testis sample, where red squares indicate regions of data acquisition. **B.** The overlay of four SWN images based on characteristic bands at 1062, 1166, 1532, and 1652 cm^{-1} where the contaminant is shown in red and surrounding tissue in green. **C.** O-PTIR spectra from the contaminant (red) and surrounding tissue (blue). **D.** O-PTIR and FTIR spectra from the contaminant. **E.** The O-PTIR contaminant spectrum matched several database composite spectra containing Cascoloid ST-56 (highest match, a milk protein- 94.3%). **F.** The FTIR contaminant spectrum matched database average spectra with percent matches ranging from 87- 89.6% with several proteins (collagen hydrolysate, Zein, human placenta extract) and Nylon –6.